

Unprecedented low twentieth century winter sea ice extent in the Western Nordic Seas since A.D. 1200

M. Macias Fauria · A. Grinsted · S. Helama ·
J. Moore · M. Timonen · T. Martma ·
E. Isaksson · M. Eronen

Received: 1 October 2008 / Accepted: 9 June 2009
© Springer-Verlag 2009

Abstract We reconstructed decadal to centennial variability of maximum sea ice extent in the Western Nordic Seas for A.D. 1200–1997 using a combination of a regional tree-ring chronology from the timberline area in Fennoscandia and $\delta^{18}\text{O}$ from the Lomonosovfonna ice core in Svalbard. The reconstruction successfully explained 59% of the variance in sea ice extent based on the calibration period 1864–1997. The significance of the reconstruction statistics (reduction of error, coefficient of efficiency) is computed for the first time against a realistic noise background. The twentieth century sustained the lowest sea ice extent values since A.D. 1200: low sea ice extent also occurred before (mid-seventeenth and mid-eighteenth centuries, early fifteenth and late thirteenth centuries), but these periods were in no case as persistent

as in the twentieth century. Largest sea ice extent values occurred from the seventeenth to the nineteenth centuries, during the Little Ice Age (LIA), with relatively smaller sea ice-covered area during the sixteenth century. Moderate sea ice extent occurred during thirteenth–fifteenth centuries. Reconstructed sea ice extent variability is dominated by decadal oscillations, frequently associated with decadal components of the North Atlantic Oscillation/Arctic Oscillation (NAO/AO), and multi-decadal lower frequency oscillations operating at ~ 50 –120 year. Sea ice extent and NAO showed a non-stationary relationship during the observational period. The present low sea ice extent is unique over the last 800 years, and results from a decline started in late-nineteenth century after the LIA.

M. Macias Fauria
Biogeoscience Institute, University of Calgary,
Calgary, AB, Canada

M. Macias Fauria · S. Helama · M. Eronen
Department of Geology, University of Helsinki,
Helsinki, Finland

A. Grinsted · J. Moore
Arctic Centre, University of Lapland, Rovaniemi, Finland

A. Grinsted
Centre for Ice and Climate, Niels Bohr Institute,
University of Copenhagen, Copenhagen, Denmark

M. Macias Fauria · M. Timonen
Rovaniemi Research Station, Finnish Forest Institute,
Rovaniemi, Finland

J. Moore
Thule Institute, University of Oulu, Oulu, Finland

J. Moore
College of Global Change and Earth System Science,
Beijing Normal University, Beijing, China

E. Isaksson
Polar Environmental Centre, Norwegian Polar Institute,
Tromsø, Norway

T. Martma
Institute of Geology, Tallinn University of Technology,
Tallinn, Estonia

M. Macias Fauria (✉)
Department of Ecology, Faculty of Biology, University
of Barcelona, Av. Diagonal 645, 08028 Barcelona, Spain
e-mail: mmaciasf@ucalgary.ca

Keywords Sea ice · Paleoclimatology · Nordic seas · Global warming · Ice core · Dendroclimatology · Svalbard · Fennoscandia · NAO · AO · Little Ice Age

1 Introduction

Arctic sea ice is a fundamental actor in the global climate system. The inhibition of heat exchange between the cold atmosphere and the warmer but ice-covered ocean in winter (Randall et al. 1998), together with its elevated albedo—typically $\sim 80\%$ in March and $\sim 50\%$ during summer melt (Robinson et al. 1992)—lead both to the Arctic Ocean being an important and highly variable component of the global heat budget. Moreover, changes in the flux of sea ice from the Arctic Ocean can have consequences for the global thermohaline circulation (Dickson et al. 1988). Sea ice affects atmospheric conditions by cold air mass formation above it (e.g., Deser et al. 2000). The climatic impacts of sea ice extent can reach systems located a long distance from the sea ice area (Serreze et al. 2007): Magnusdottir et al. (2004) and Alexander et al. (2004) suggested that sea ice extent in the North Atlantic can influence the mode of the North Atlantic Oscillation (NAO) and Singarayer et al. (2006) reported that changes in sea ice extent promote alterations in atmospheric circulation and precipitation patterns that extend to mid-latitude storm tracks.

Large changes have occurred in the Arctic during the last four decades (Serreze et al. 2000; Morison et al. 2000; ACIA 2004; Serreze and Francis 2006b). These include (a) increases of surface air temperatures (SAT) over most of Eurasia and North America; (b) extended periods of low sea level pressure (SLP) over the Arctic Ocean; (c) increase of the inflow and temperature of warm and saline Atlantic water into the Arctic Ocean; (d) thinning of the cold halocline layer that insulates the cold- and low-salinity surface water of the Arctic Ocean from the warm and saline Atlantic water underneath (Grotefendt et al. 1998); (e) increase of Siberian rivers discharge (Peterson et al. 2002); (f) general warming of the Arctic soils and permafrost (Lemke et al. 2007; although the short length of the timeseries suggests caution in this respect); (g) decreases of sea ice thickness (Rothrock et al. 1999, 2008; Tucker et al. 2001; Lindsay and Zhang 2005; Maslanik et al. 2007a), and (h) reductions of sea ice area and extent, both in summer (e.g., Serreze et al. 2003, 2007; Stroeve et al. 2008) and in winter (e.g., Comiso 2006; Comiso and Nishio 2008; Comiso et al. 2008; Deser and Teng 2008; Parkinson and Cavalieri 2008).

Changes in sea ice thickness and extent have been attributed to both (1) intrinsic strong decadal to interdecadal oscillations in the Arctic climate system linked with the North Atlantic Oscillation/Arctic Oscillation (NAO/AO; Hurrell 1995; Thompson and Wallace 1998, 2000;

Thompson et al. 2000; Deser et al. 2000) together with the dynamics of the thermohaline circulation (e.g., Dickson et al. 2000; Polyakov and Johnson 2000; Deser et al. 2000; Polyakov et al. 2002, 2003a, b, 2004; Rigor et al. 2002), and (2) external forcing from enhanced greenhouse gas-caused global warming in the Arctic (e.g., Vinnikov et al. 1999; Rothrock and Zhang 2005; Comiso 2006; Winton 2006; Serreze and Francis 2006a; Stroeve et al. 2007; Serreze et al. 2007). The extremely low values of sea ice extent (especially in summer minimum sea ice but also in winter maximum sea ice) in recent years have led to a consensus that the cause is a combination of natural variability in the coupled ice–ocean–atmosphere system and growing radiative forcing associated with rising concentrations of atmospheric greenhouse gases (Serreze et al. 2007; Maslanik et al. 2007a; Stroeve et al. 2008). According to this view, sea ice extent during the late 1980s and early 1990 was largely governed by extreme and persistent positive NAO/AO situations, which replaced previously large areas of thick multiyear ice with thin young (and hence more vulnerable) ice and also created larger regions of open water (e.g., Zhang et al. 2008; Stroeve et al. 2008). The return of the NAO/AO to a neutral state in the late 1990s did not stop or slow down the decline in sea ice during the early twenty-first-century (e.g., Overland and Wang 2005; Comiso 2006; Serreze and Francis 2006a, b), suggesting that sea ice might have reached a tipping point where strong positive feedback mechanisms such as those associated with ice-albedo and open water formation efficiency are accelerating the thinning and retreat of pre-conditioned vulnerable Arctic sea ice (Comiso et al. 2008; Deser and Teng 2008; Parkinson and Cavalieri 2008; Zhang et al. 2008). Nonetheless, most environmental records in the Arctic are short and cover just a few decades, making it difficult to assess the present in terms of long-term variability. For example, observations of Arctic sea ice from satellite passive microwave radiometer data on which most of these studies are based started in 1979.

The Western Nordic Seas—Greenland, Norway and Iceland Seas, i.e., roughly the sea region between Greenland and 10°E , Fig. 1—are of major importance for the oceanography of the Arctic region, as they constitute the area with the greatest sea ice variability, coinciding with the sea ice feature known as ‘Odden’, a tongue of sea ice that episodically advances rapidly northeastward into the Greenland sea from the edge of the ice pack near 10°W between 72° and 74°N . At least one such advance occurs during most winters (Deser et al. 2000). The largest oceanic and atmospheric heat inputs to the Arctic Ocean arise via the warm and saline North Atlantic current, which enters the Nordic Seas and splits, becoming the West Spitsbergen Current towards Fram Strait and the Barents Sea branch (Grotefendt et al. 1998; Dickson et al. 2000; Fig. 1). Part of the ice formed in the Arctic Ocean is

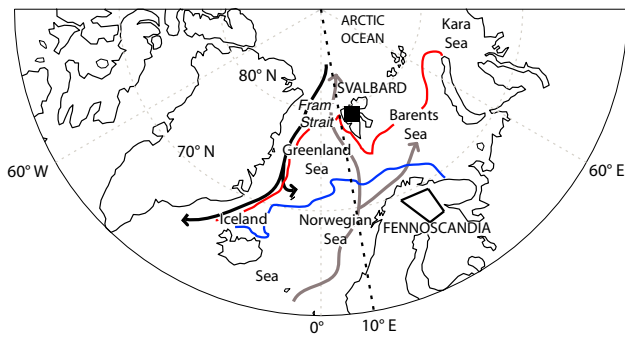


Fig. 1 Map of the Nordic Seas, which comprise the Iceland, Greenland, Norwegian, Barents, and Western Kara Seas. April or maximum sea ice extent was reconstructed for the Western Nordic Seas, i.e., the area west of 10°E (Vinje 2001; dashed black line), comprising the Iceland, Greenland and Norwegian Seas. Ice edge locations are shown to give a measure of sea ice variability for the northernmost (red continuous line, 1995) and the southernmost (blue continuous line, 1866) years in the historical record (1864–1998, Vinje 2001). Ice core record location (Lomonosovfonna) is displayed as a black square in the Svalbard Archipelago. Forest-tundra ecotone area where the locations for the tree-ring chronology are displayed as an empty polygon in Fennoscandia. The inflow of warm and saline Atlantic water into the Arctic Ocean from the North Atlantic Ocean is indicated by continuous grey thick arrows, whereas sea ice export routes through Fram Strait into the Greenland Sea are depicted as continuous black arrows (according to Grotfendt et al. 1998)

exported through Fram Strait into the Greenland Sea and to the North Atlantic, where the ice and freshwater play a role in the global thermohaline circulation (Rigor et al. 2002) via deep water formation (Manabe et al. 1992; Schaeffer et al. 2004; Moore 2006).

A useful and robust measure of winter season severity is the maximum ice extent, which reflects the net effect of winter dynamics and the northbound warmer currents (Vinje 2001). In practice, before the satellite era, this was impossible to determine as the date of maximum ice extent varies from year to year. An excellent proxy for maximum extent is the sea ice extent in April, when sea ice is very close to its maximum and varying rather slowly compared with other months of the winter and spring (e.g., Parkinson et al. 1999). A yearly timeseries of historical April sea ice extent in the Western Nordic Seas for the period 1864–1998 was obtained by using a combination of ship, aircraft reconnaissance flights and satellite observation data (Vinje 2001; Shapiro et al. 2003; Fig. 2a). The data shows a 46% reduction of ice extent in the Western Nordic Seas over the whole period, largely attributed to a decreased frequency of the Odden ice feature in the Greenland Sea (Vinje 1976, 2001). The largest sea ice reduction occurred before 1900, that is, prior to the early twentieth century warming of land surface stations around the Arctic Ocean (~ 1900 –1940) and coincident with increased sea surface temperatures (SSTs) (e.g., Vinje 2001). Earlier records of sea ice extent in the area are discontinuous (e.g., Vinje 1999; Divine and Dick 2006).

In this paper we present a reconstruction of the decadal to centennial variability of maximum sea ice extent in the Western Nordic Seas for the period 1200–1997 obtained by combining ice core $\delta^{18}\text{O}$ records from Svalbard and tree-ring width chronologies from the timberline in northern Fennoscandia (Fig. 1). We show that the reduced twentieth century sea ice extent is uniquely persistent compared to the last eight centuries. Reconstructed sea ice extent variability is dominated by decadal and multidecadal oscillations resembling the poorly defined low frequency oscillation (LFO), and a NAO-decadal component previously reported to control sea ice variability in Russian Arctic Seas—Kara, Laptev, East Siberian and Chukchi Seas (Polyakov et al. 2003b).

2 Data and methods

In 1997, a 121-m ice core was retrieved from Lomonosovfonna, the highest ice field in Spitsbergen, Svalbard (1,250 m.a.s.l.). The core was sampled for $\delta^{18}\text{O}$ with 5 cm resolution (Isaksson et al. 2001), and dated using a combination of known reference horizons and glacial modelling (Kekonen et al. 2005). The period covered by the ice core is A.D. 1200–1997. This ice core has been previously reported to exhibit significant low frequency variability and links with climate and sea ice over the last 400 years (e.g., Isaksson et al. 2005). The records of $\delta^{18}\text{O}$ were found to be consistent with the temperature record from Longyearbyen (Svalbard; Isaksson et al. 2001, 2003, 2005) and the historical sea ice record from the Western Nordic Seas over the last 150 years at multiyear resolution (Table 1). All series were standardized by subtracting the average value of the series from each value and dividing it by the series standard deviation. A 5-year cubic spline smoothing function (Cook and Peters 1981) was applied to the standardized timeseries in order to eliminate high-frequency information that may be corrupted by dating errors in the ice core—especially in the early part of the record—and by complications caused by the limited summer melting (Virkkunen et al. 2007), which does not penetrate deeper than 5 years from the surface of the snow pack (Pohjola et al. 2002, Moore et al. 2005). Comparison of the sulphate record in the core with dates of known volcanic eruptions shows that the dating is accurate within a range of 2–5% between 1250 and 1991 (Moore et al. 2006). For this reason, our reconstruction does not attempt to reproduce interannual changes (high-frequency variability) and is mainly restricted to the decadal to interdecadal variability.

The long ring width chronology of Scots pine (*Pinus sylvestris* L.) from the forest-tundra ecotone in northern Finnish Lapland has been described in Eronen et al. (2002) and Helama et al. (2002). The whole chronology consists of

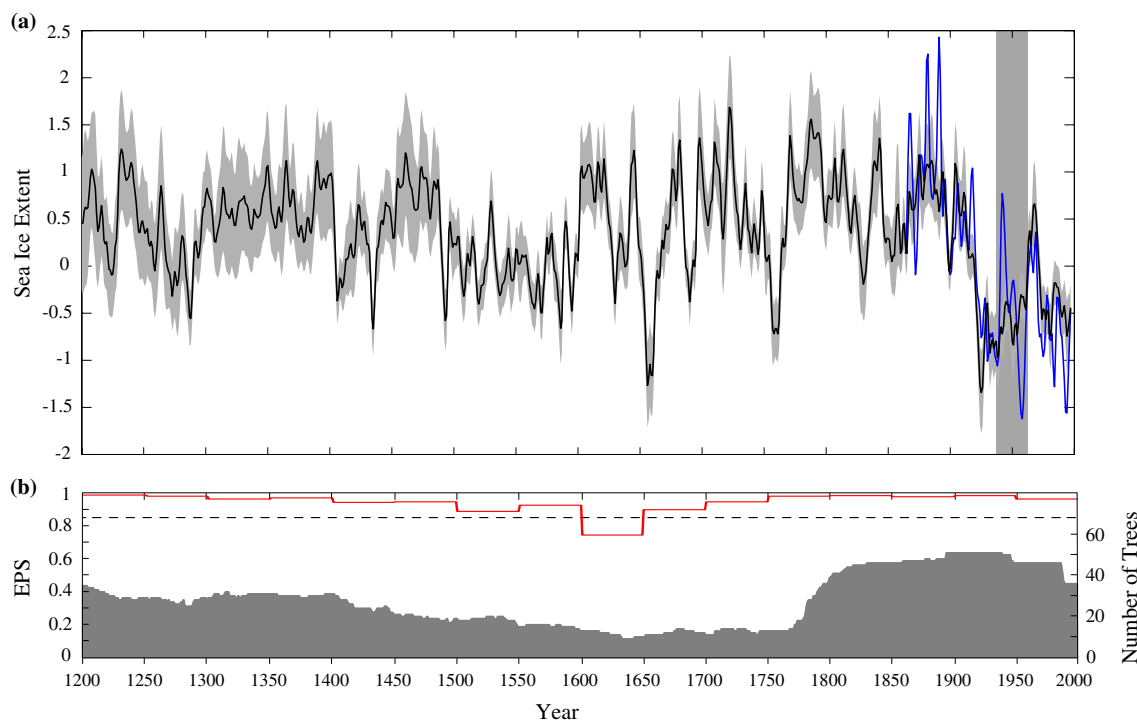


Fig. 2 **a** Blue line: 5 year smoothed historical maximum sea ice extent in the Western Nordic Seas (Norway, Iceland and Greenland Seas; Vinje 2001) during 1864–1997. The period 1940–1959, obtained mainly from interpolation due to abundant missing data (see “Data and methods”), is highlighted by a grey shaded rectangle; black line: multiproxy reconstruction of sea ice extent in the Western Nordic Seas during 1200–1997; grey shaded area: area within the

95% confidence interval of the reconstruction (see “Data and methods” for computation); **b** red thick line expressed population signal (EPS; Wigley et al. 1984) statistics of the tree-ring chronology averaged over 50 year periods; black dashed line threshold EPS value of 0.85, indicative of good reliability in chronology replication (Wigley et al. 1984); grey shaded area number of trees per year used in the tree-ring chronology

more than 250 samples from living pines and over 1,700 samples of sub-fossil pines that form an unbroken pine chronology about 7,500 years long, dated to an accuracy of 1 year, and has been extensively used in temperature reconstructions of Northern Fennoscandia (e.g., Eronen et al. 2002; Helama et al. 2002). For this study, we limited our chronology to the period A.D. 1200–1997, which totals 225 trees, both living and sub-fossil (sample depth = 30 ± 14 trees per year; Fig. 2b). Cross-dating of the ring width samples was verified using the computer program COFECHA (Holmes 1983). The individual tree-ring measurement series were detrended using the regional curve standardization (RCS) procedure (Erlandsson 1936; Fritts 1976; Briffa et al. 1992, 1996), specifically designed to preserve low frequency variability in tree-growth chronologies. The expressed population signal (EPS) statistic quantifies the similarity between the averaged chronology (the mean of a finite number of sample indices) and the theoretical population chronology (Wigley et al. 1984). A threshold EPS value of 0.85 has been widely accepted in tree-ring studies as indicative of good reliability in chronology replication and good signal strength (Wigley et al. 1984). Given a mean inter-series correlation of the RCS-indices (series length = 185 ± 53 year) of 0.34, a

minimum of 12 trees was needed for EPS statistics >0.85 . This requirement is satisfied in the full chronology period, with a minor exception in a short period in mid-seventeenth century, when 9–11 trees per year were available, with a resulting EPS statistic of 0.74 (Fig. 2b). The resulting chronology showed strong correlation with the historical sea ice record of the Western Nordic Seas (Table 1), especially at multiyear resolution. As with the $\delta^{18}\text{O}$ time-series, the tree-ring chronology was smoothed with a 5-year cubic spline smoothing function.

A number of studies have demonstrated that both ice cores and tree-rings can capture climate on very large spatial scales (e.g., Moberg et al. 2005; Jones and Mann 2004; Vinther et al. 2003). Sea ice extent in the Western Nordic Seas, the timberline area in northern Fennoscandia, and Svalbard climate are largely forced by the same large-scale climate variations. Svalbard and the Nordic Seas ice edges are in a key region for the Atlantic overturning (Fig. 1). The warm mild climate in northern Scandinavia is a direct consequence of this overturning. Furthermore, historical maximum sea ice extent in the Western Nordic Seas and the proxy data used in the reconstruction display a strong and spatially coherent relationship with annual SSTs in the region (Fig. 3): whereas the tree-ring chronology shows high

Table 1 Reconstruction statistics

Period	Proxy data	Unfiltered		5 year smoothed		High-pass filtered	
		r	r^2	r	r^2	r	r^2
1864–1997 ^a	$\delta^{18}\text{O}$ ice core chronology	0.36**	0.13**	0.48**	0.23**	0.14	0.02
1864–1997 ^b	Tree-ring chronology	0.60***	0.36***	0.73***	0.53***	0.10	0.01
Full calibration period	Full calibration statistics	Verification statistics ^c		R^2	r^2		
		RE	CE				
1864–1997	0.59***	0.70***	0.25**	0.62**	0.58**		

Upper correlation coefficient (r) and explained variance (r^2) between the historical maximum sea ice extent in the Western Nordic Seas. Correlations are shown for *unfiltered* (yearly resolution), *5 year smoothed*, and *High-pass filtered* timeseries.

High-pass filtered series were calculated by subtracting the unfiltered from the smoothed timeseries, and give a measure of the high-frequency agreement between the series.

Significance of all statistics was calculated taking into account autocorrelation in the timeseries (see “Data and methods”).

Lower calibration-verification statistics for the multiproxy reconstruction: *full calibration* R^2 refers to the variance explained by the model over the period 1864–1997: $\text{SI}_{(t)} = 0.33 - 0.58\text{TR}_{(t-1)} - 0.27\delta^{18}\text{O}_{(t-2)}$ (see “Data and methods”).

Verification statistics: *RE* reduction of error; *CE* coefficient of efficiency; R^2 variance explained by the model obtained from the calibration period 1960–1997 over the observed values for the calibration period 1960–1997; r^2 variance explained by the model obtained from the calibration period 1960–1997 over the observed values for the verification period 1864–1939.

** $p < 0.01$

*** $p < 0.001$

^a The $\delta^{18}\text{O}$ ice core chronology

^b Northern Fennoscandia tree-ring chronology

^c Calibrated: 1960–1997; verified against 1864–1939

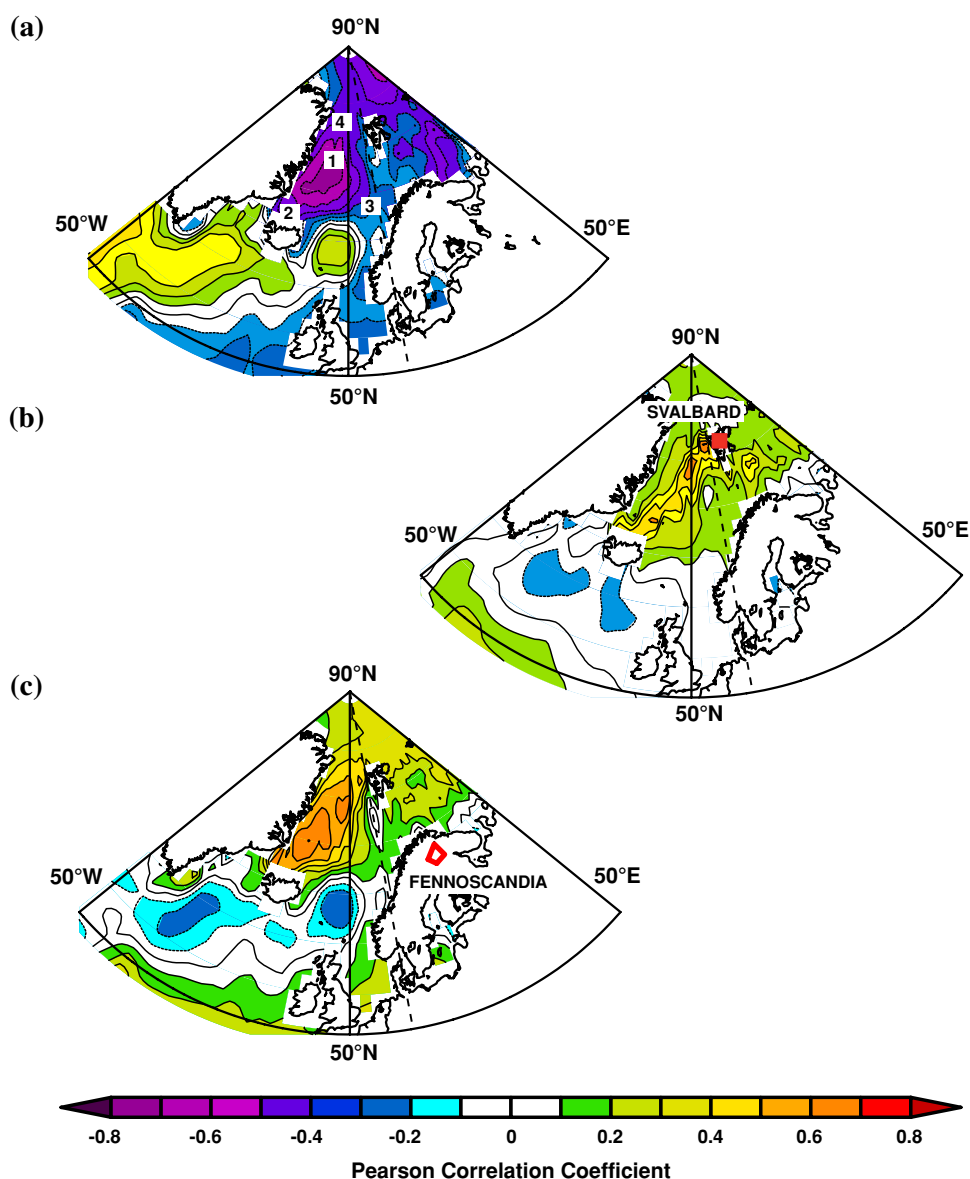
correlations with SST over the whole reconstructed area, the correlations between the ice core $\delta^{18}\text{O}$ timeseries and SST are high right along the typical location of the sea ice edge. Such spatially coherent patterns provide further indirect evidence of the strong coupling between the timeseries of proxy data used in the reconstruction and the historical record of sea ice extent in the Western Nordic Seas.

As we were dealing with autocorrelated data—5 year smoothed timeseries—we computed the significance of Pearson correlation and of the climate reconstruction statistics (reduction of error, RE; and coefficient of efficiency, CE; Lorenz 1956; Fritts 1976; Briffa et al. 1988) using a combination of autoregressive (AR) modelling and Monte-Carlo methods. For any given pair of series, the AR model parameters of both were calculated using Burg’s method (Burg 1978). The best AR model (i.e., the best model order) for each timeseries was selected using the Akaike Information Criterion (Akaike 1974). Once an AR model of each series was estimated, 10,000 pairs of surrogate series with the same AR characteristics were generated and their corresponding statistics (Pearson correlation, RE, or CE) calculated: the empirical probability distribution of the statistic value was then easily calculated and, hence, its significance. This method is robust as it accounts for persistence in the timeseries. Table 2 shows the order of the AR model used for each timeseries.

The high autocorrelation of proxy data can be exploited by considering the maximum sea ice extent in year t to be a function of tree-growth and $\delta^{18}\text{O}$ values in both the year concurrent with the proxy series, and also potentially up to n years prior and after the concurrent year (Fritts 1962; Briffa et al. 1988). Physically speaking, albedo feedback and ice thickness can largely delay the effects of climate on sea ice extent, delaying in turn the relationship between proxy and reconstructed variables. Further, although pines’ growth starts and ends during the growing season of year t , the influence of climate in previous years modifies the trees’ response to climate in later years due to arboreal physiology, a phenomenon known as physiological preconditioning (Fritts 1976). We thus applied a model structure including 2-year lagging ($t + n$) and 2-year leading ($t - n$) predictors in the linear multiple regression used to estimate this relationship. That is, there were ten candidate predictors: five corresponding to the tree-ring width chronology and five to the ice core $\delta^{18}\text{O}$ record ($t - 2$, $t - 1$, $t = 0$, $t + 1$, and $t + 2$ for each proxy variable). The final model was chosen using a stepwise selection procedure with entry and removal criteria for retention of predictors set at an F -statistic probability of less than 0.05 and 0.10, respectively (e.g., Lindholm 1996; Helama et al. 2002).

According to uniformitarian principle, the relationship between environmental and proxy data characteristics

Fig. 3 **a** Correlation between maximum sea ice extent in the Western Nordic Seas and annual sea surface temperatures (SST); 1 Greenland Sea, 2 Iceland Sea, 3 Norwegian Sea, 4 Fram Strait. Sea ice was reconstructed for the region lying west of 10°E (dashed black line); **b** correlation between the $\delta^{18}\text{O}$ ($t - 2$) ice core record from Lomonosovfonna (Svalbard) and annual SST; red square location of the ice core; **c** correlation between the timberline tree-ring width chronology ($t - 1$) and annual SST; red empty polygon displays the Northern Fennoscandia timberline area. Data and software for the figure obtained from the NCEP/NCAR Reanalysis Project (Kalnay et al. 1996). Period: 1948–1997. The use of lag comes from the model used in the reconstruction: $SI_{(t)} = 0.33 - 0.58TR_{(t-1)} - 0.27O_{(t-2)}$, where SI is Sea Ice extent, TR are tree-ring indices, and O is $\delta^{18}\text{O}$ ice core record (see “Data and methods”)



(tree-ring width and ice core $\delta^{18}\text{O}$ records in this study) should have been the same in the past as in the present (Fritts and Swetnam 1989). If this principle does not hold, conclusions concerning the past cannot be made. This is why multiple linear regression is generally computed for a calibration period with some of the observational values (sea ice extent in this study) withheld to assess the veracity of the relationship with independent data (the verification period; e.g., Fritts 1976; Jones et al. 1998). Once the statistics (r^2 , RE and CE) were tested and found to be significant ($p < 0.05$), sea ice extent was reconstructed using the whole period of observed values as a final calibration period. Successful verification supports the validity of uniformitarian principle and therefore the validity of the reconstruction (Fritts 1976). Further, confidence intervals for the reconstruction were then calculated from the

autoregressive structure of the residuals of the multiple regression computed over the calibration period 1864–1997, and were based on generating 10,000 surrogate series of residuals with the same AR structure as the residuals from the reconstruction regression. This method gave more conservative results than the use of resampling with replacement in the calculation of the confidence intervals.

The period of observed sea ice extent covering 1940–1959 includes some gaps in the data due to World War II (Divine and Dick 2006) and much of it is largely based on interpolation of the few available observations (Løyning et al. 2003; Divine, personal communication). For this reason, we did not include it in the calibration-verification procedure. We thus calibrated a multiple linear regression model on the period 1960–1997 that was verified against 1864–1939 data (e.g., Mann et al. 2005). On the basis of

Table 2 Autoregressive/Monte-Carlo modelling

Timeseries	AR order						
	0	1	2	3	4	5	6
TR	1.000	-2.054	2.109	-1.744	1.187	-0.605	0.135
$\delta^{18}\text{O}$	1.000	-1.872	1.779	-1.328	0.848	-0.347	-
SI	1.000	-2.128	2.242	-1.640	0.812	-0.241	-
CI	1.000	-1.926	2.056	-1.620	0.917	-0.272	-
mc iterations	10 ⁴						
Max AR order	30						

Autoregressive coefficients and stochastic terms used in the modelling of the significance of the reconstruction statistics for each timeseries used in the study

TR tree-ring width from northern Fennoscandia; $\delta^{18}\text{O}$ ice core record from Lomonosovfonna; *SI* sea ice extent records in the Western Nordic Seas (Vinje 2001); *CI* confidence intervals of the reconstruction, i.e., autoregressive structure of the residuals of the multiple regression (see “Data and methods”); *mc iterations* number of Monte-Carlo surrogate series for the calculation of the significance; *max AR order*: maximum autoregressive order allowed in the AR modelling

these calibrations, the model using tree-ring width at $t - 1$ and ice core $\delta^{18}\text{O}$ at $t - 2$ was selected. Output from this model using the period 1960–1997 was significantly correlated with observed values during the verification period 1864–1939 ($r^2 = 0.58$, $p < 0.01$; Table 1). RE and CE statistics were positive and significant at $p < 0.001$ and $p < 0.01$, respectively (Table 1), indicating skill of the model in estimating sea ice extent outside the calibration period. The significance of both RE and CE shows that the quality of the reconstruction is high and cannot be simply due to similarity of trend. To further test this possibility, the regression was repeated after linear detrending of the timeseries, being significant ($r^2 = 0.30$, $p < 0.0001$), as well as the RE and CE statistics (RE = 0.42, $p < 0.001$ and CE = 0.31, $p < 0.0001$). We then used the whole period 1864–1997 to produce:

$$\text{SI}(t) = 0.33 - 0.58\text{TR}_{(t-1)} - 0.27\text{O}_{(t-2)} \quad (1)$$

where $\text{SI}(t)$ are the standardized (mean = 0, standard deviation = 1) historical Western Nordic Seas April sea ice extent, $\text{TR}_{(t-1)}$ are the 1-year previous tree-ring width index, and $\text{O}_{(t-2)}$ are the 2-year previous standardized $\delta^{18}\text{O}$ ice core values. As previously suggested, there are physically plausible mechanisms that can lead to temporal lags in the relationship between the variables and climate that result in Eq. 1: while $\delta^{18}\text{O}$ in ice cores most likely records temperature occurring in the current year, physiological pre-conditioning in trees can easily delay the effect of climate on tree-growth by 1 year (e.g., Fritts 1976), whereas albedo and sea ice thickness feedbacks may further delay the effects of climate on sea ice another year. However,

given the fact that 5 year smoothed timeseries were used, the selection of these particular lags can also be considered arbitrary as they are out of the series’ time resolution. SI values were then scaled to km^2 according to the mean and standard deviation of the observed sea ice extent during the full period 1864–1997 to give the reconstructed sea ice extent. Output from this model was highly correlated with the observed data for 1864–1997 ($r^2 = 0.59$; $p < 0.001$; Table 1) and for both early (1864–1939) and late (1960–1997) periods ($r^2 = 0.64$ and $r^2 = 0.59$, respectively).

We used a Morlet wavelet approach (Torrence and Compo 1998; Jevrejeva et al. 2003; Grinsted et al. 2004) to evaluate the stationarity of the reconstructed sea ice variability in the time–frequency domain and to find out if dominant low-frequency modes of variability control or have controlled sea ice variability in the region. The wavelet transform expands a timeseries into time–frequency space, representing its frequency content while still keeping the time description parameter. Our analysis involved Continuous Wavelet Transform (CWT), a common and powerful tool for analyzing intermittent oscillations in a timeseries. Such analysis has data-boundary edge artifacts that are accounted for by defining a cone of influence (COI), outside which edge effects can be ignored. Spectral characteristics of the reconstructed sea ice variability were also estimated using the multi-taper approach (MTM; Ghil et al. 2002).

3 Results and discussion

The Western Nordic Seas maximum sea ice extent reconstruction (Eq. 1) explained 59% of the variance in sea ice extent in the Western Nordic Seas (Table 1), successfully capturing the main features of historical sea ice extent variability since 1864 (Fig. 2a; Vinje 2001; Shapiro et al. 2003), namely:

- (1) A sharp decrease in late nineteenth and early twentieth centuries. Such a reduction corresponds to the end of the Little Ice Age (e.g., Overpeck et al. 1997) and has been related to changes in SSTs before 1900 (Vinje 2001) and atmospheric warming driven by enhanced atmospheric and ocean heat transport from the North Atlantic into the region from 1900 to 1940 (Vinje 2001; Bengtsson et al. 2004).
- (2) Minima in sea ice extent in the 1920s and 1930s, coincident with high recorded temperatures in the Arctic (Nordli and Kohler 2003; Polyakov et al. 2003a; ACIA 2004).
- (3) A recovery from the 1940s to late 1960s, coinciding with a general cooling in the region (Polyakov et al. 2003a; ACIA 2004). This increase in sea ice extent

was partly masked in the sparse observations during the period 1940–1959 but appears clearly in the reconstruction (Fig. 2a).

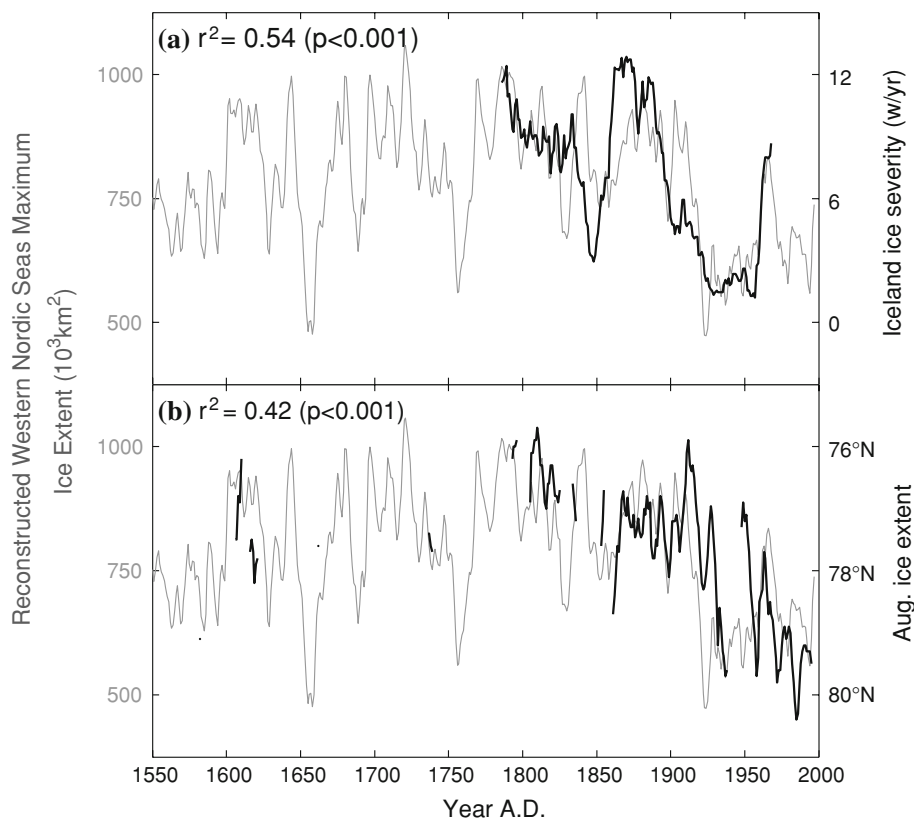
- (4) A decrease in sea ice extent from then until the end of the twentieth century, widely reported to be the general trend in sea ice extent over the whole Arctic Ocean and Arctic marginal seas (Serreze et al. 2000, 2007; Dickson et al. 2000; Deser et al. 2000; Rigor et al. 2002; Polyakov et al. 2003b; Nghiem et al. 2006; Comiso 2006).

3.1 Comparison with other sea ice records

The twentieth century supported the smallest sea ice extent in the Western Nordic Seas of the whole reconstructed period (Fig. 2a): moreover, the local maximum of sea ice extent reached in the 1960s is not especially high when compared with sea ice over the last eight centuries. Although proxy versus sea ice extent relationships proved to be stable over the observational period, it is still possible that this assumed stationarity did not hold constant over the reconstruction period. Such a limitation is common to most paleo-reconstructions but the likelihood of this can be further minimized through the comparison of the reconstructed timeseries with other related datasets of independent origin. Occasional observations of minimum (August) sea ice extent between ~ 1600 and 1850 (Vinje 1999) are

consistent with our maximum sea ice extent reconstruction (Fig. 4b). Overall, sea ice extent was large from the seventeenth to the nineteenth centuries, which agrees well with the occurrence of the Little Ice Age (LIA) in the area (e.g., Fischer et al. 1998; Hammer et al. 2001). Several short duration warm events occurred during this period: the mid-eighteenth century contains a decade and a half with low sea ice extent. Mid-eighteenth century warmth has been reported before (Overpeck et al. 1997; Vinje 2001; Isaksson et al. 2005; Divine and Dick 2006). A rapid cooling followed that led to very large ice extent at the end of the eighteenth and during the nineteenth centuries. This increase in sea ice extent was sufficiently widespread to be recorded in the Icelandic sea ice (e.g., Lamb 1977; Ogilvie 1992), which shows high agreement with our reconstruction (Fig. 4a). Another warm spell occurred in mid-seventeenth century, with values as low as those in the twentieth century, but not as long lasting. This particular event should, however, be treated with caution, as it corresponds to the period with low replication in the tree-ring chronology (Fig. 2b). Sea ice extent was smaller before the LIA: the sixteenth century was a period of sustained low sea ice extent, agreeing with reported warm temperatures in Europe (e.g., Briffa et al. 2004), whereas the period covering the thirteenth to the fifteenth centuries exhibited larger sea ice areas, but with overall lower values than during the LIA, and with some periods of lower sea ice

Fig. 4 Reconstructed maximum sea ice extent in the Western Nordic Seas (grey line) versus **a** 15 year smoothed Iceland Sea sea ice severity (in weeks per year, week/year; black line Lamb 1977) and **b** latitude-based database of August sea ice extent in the Nordic Seas (black line; Vinje 1999). Significance levels were calculated taking into account autocorrelation in the timeseries (see “Data and methods”)



extent spanning a few decades during A.D. 1270–1300 and A.D. 1400–1430.

Further, Fig. 4 illustrates delayed dynamics between sea ice extent and climate: the post-LIA decline in sea ice coverage started earlier in the Icelandic record (~ 1880 ; Fig. 4a), followed by the decline in maximum sea ice extent in the Western Nordic Seas (late nineteenth–early twentieth century). The decline in August (minimum) sea ice extent in the Western Nordic seas occurred later (~ 1930 s; Fig. 4b). The Iceland Sea is located at the southernmost sea ice limit and is therefore mostly composed of very young ice, which rapidly responds to changes in climate. April (maximum) sea ice extent is a mixture of both multi-year ice and the ice formed in that particular winter. Multiyear ice can in general better survive warming than young ice and therefore has a longer response time. We speculate that the relative lags in sea ice decline at the end of the LIA can be explained by the different degrees of multiyear ice present at these locations and times.

3.2 Wavelet decomposition and MTM spectrum

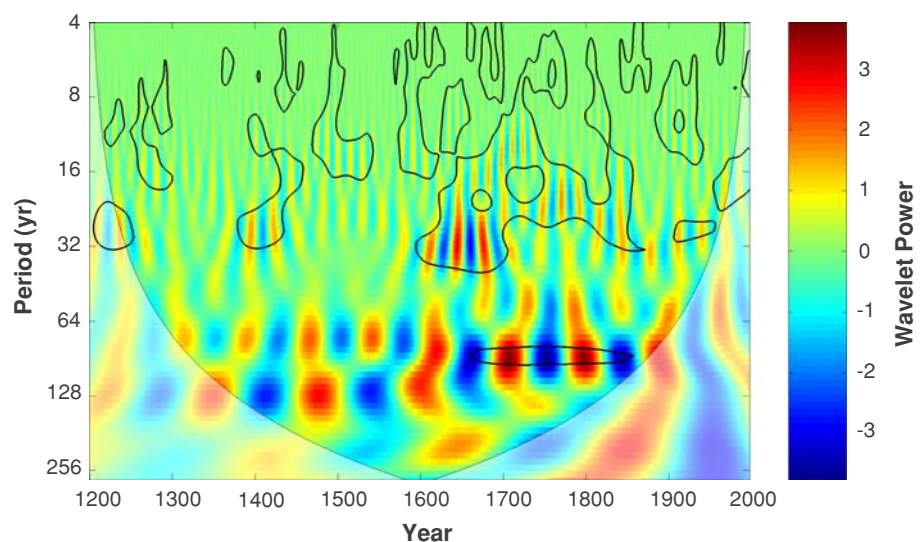
The wavelet spectrum of the full reconstruction (Fig. 5) showed significant energy spread over a wide band from ~ 7 to 32 years, with strong persistence and power at ~ 16 –32 years, especially from the seventeenth to mid-nineteenth century. The ~ 50 –120 year band also showed high variability and power, centred at ~ 70 –90 years from late sixteenth century to the present. Power in the ~ 50 –120 year band separated into two main centres of variability before then (although not significant) with the main one at somewhat lower frequencies (~ 128 year) and high power also at the ~ 70 year band. MTM spectrum further confirmed these results: when computed over the whole reconstructed period (1200–1997; Fig. 6a), several spectral

peaks were found at frequencies ranging from 13 to 32 years, plus a significant peak centred at 93 year, coincident with the ~ 70 –90 year range of high variability found in the wavelet analysis. MTM spectrum post-late sixteenth century (1561–1997; Fig. 6c) showed significant peaks within both the ~ 7 –32 year and ~ 70 –90 year bands previously identified in Fig. 5, whereas significant peaks were found only at the higher frequency band in the pre-late sixteenth century MTM (1200–1560; Fig. 6b). The two main centres of low frequency variability in Fig. 5 were not significant in this case, in agreement with the wavelet analysis. Our results are consistent with those reported by Divine and Dick (2006) for documentary evidence on sea ice in the same region since 1750. The ~ 50 –120 year oscillation accounts for most of the main interdecadal sea ice extent oscillations seen in the historical record, that is: (1) large extent in mid-late nineteenth century, (2) drop to low values towards the 1930s, (3) higher values in the 1960s and (4) drop again thereafter. However, caution is advised in this respect, as the twentieth century power at these low frequency scales is inside the COI and thus affected by edge effects. Finally, and also inside the COI, spectral power is seen at centennial scales (~ 256 year) that accounts for the generalized large sea ice extent of the late eighteenth and the nineteenth centuries (peak of the LIA) and the overall downward trend observed since late nineteenth and during the twentieth centuries (current Arctic warming).

3.3 Low frequency variability

Low-frequency interdecadal variability (~ 50 –80 year), previously defined as LFO, is seen in a large part of the observed environmental variability in the Arctic during the last century and a half, including sea ice variability (e.g.,

Fig. 5 Continuous wavelet power spectrum of the normalized timeseries of reconstructed maximum sea ice extent in the Western Nordic Seas for the period 1200–1997. The *thick black contour* designates the 5% significance level against red-noise. The cone of influence, which defines where edge effects are important, is shown as a *lighter shade*. *Red areas* indicate large sea ice extent at a given frequency and *blue areas* indicate low sea ice extent at a given frequency



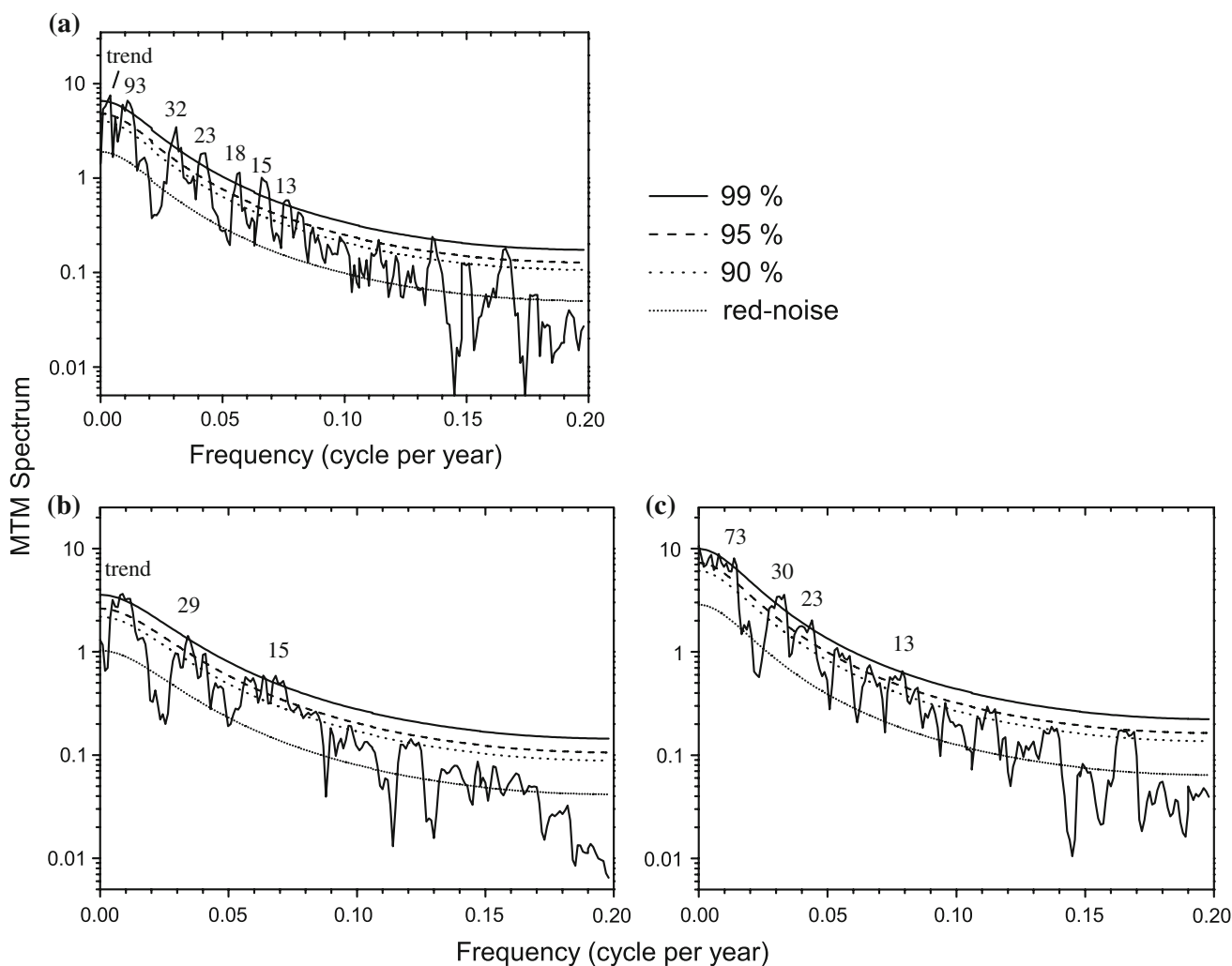


Fig. 6 Spectral characteristics of reconstructed sea ice variability, estimated as spectrum by multi-taper method (Ghil et al. 2002) for the periods 1200–1997 (a), 1200–1560 (b), and 1561–1997 (c). The estimated red-noise background and the associated significance levels

are shown by the *smooth curves*. Spectral peaks found significant at the 99% level are shown as their estimated periodicities in years. The term ‘trend’ refers to wavelengths approaching the length of the study interval

Polyakov et al. 2003a; Divine and Dick 2006), and has been linked to the thermohaline circulation in the North Atlantic (Polyakov and Johnson 2000) and to multidecadal variability in Atlantic Ocean SSTs (Atlantic Multidecadal Oscillation—AMO; Delworth and Mann 2000; Polyakov et al. 2004). However, direct observational evidence on these long cycles is very limited, and modelling using coupled GCMs shows rather ill-defined power on these timescales (Knight et al. 2005). It has been suggested that the AMO is in fact an insignificant player in Atlantic SST and the well-documented apparent cycle over the last century and a half is actually a superposition of globally warming temperatures and regional cooling due to mid-twentieth century anthropogenic aerosols (Mann and Emanuel 2006). However, our results (Figs. 5, 6a) suggest that sea ice variability has exhibited oscillations in the band defined as the LFO or AMO during the last eight centuries.

Results also suggest that low frequency variability was centred at lower frequencies before the seventeenth century (~ 128 year, albeit non-significant) than after it (~ 70 – 90 year), which again raises the issue of whether the low frequency signal is a true oscillation caused by a simple physical mechanism or is some combination of different forcing factors.

Variability at these low frequency bands also coincides with long-term variations in solar activity (Gleissberg cycles; Gleissberg 1944; Ogurtsov et al. 2002). However, the physical mechanisms of solar influence on Earth’s climate are not yet fully explained, and GCM simulations suggest that the influence of solar activity on tropospheric temperature, while accounting for some variability, does not account for the magnitude of the observed variability, especially on a global scale and in the presence of large anthropogenic trends (Cubasch et al. 1997; Lockwood and

Fröhlich 2007). Thus, it seems plausible to attribute sea ice low frequency variability to a (likely non-linear) combination of extrinsic (that is mainly solar forcing and volcanic aerosol cooling) and intrinsic Atlantic thermohaline circulation variability, which together act on the large-scale atmospheric circulation patterns.

3.4 Multi-year and decadal variability

This section will first extend on the correlation between the reconstructed sea ice extent in the Western Nordic Seas and the North Atlantic Oscillation/Arctic Oscillation system, and close with evidence of the non-stationary nature of this relationship. Decadal-scale variability in sea ice extent (~ 7 –32 year; Figs. 5, 6) has been linked to the low-frequency component of the NAO/AO in the Arctic Ocean and Arctic Eurasian seas close to the North Atlantic Ocean (Dickson et al. 2000; Deser et al. 2000; Polyakov et al. 2003b). Positive NAO/AO situations are related to decreased SLPs over the Arctic region—with a minimum over Iceland—and a northeastward extension of the Atlantic storm track to Greenland, Iceland, Norway and Barents Seas, causing major increases in cyclone activity in the area and thus increased heat flux over the region (Serreze et al. 1997; Alexandersson et al. 1998). As mentioned in the “Introduction”, the decadal variability of the NAO/AO strongly affected Arctic sea ice variability in the second half of the twentieth century, especially in the 1980s and early 1990s (Deser et al. 2000; Dickson et al. 2000; Polyakov and Johnson 2000; Rigor et al. 2002). In the mid-1990s the effects of greenhouse gas-induced global warming and the ice-albedo feedback started to override the effects of these oscillations (Serreze et al. 2007; Comiso et al. 2008; Deser and Teng 2008; Stroeve et al. 2008). Annual records of Icelandic SLP back to 1820

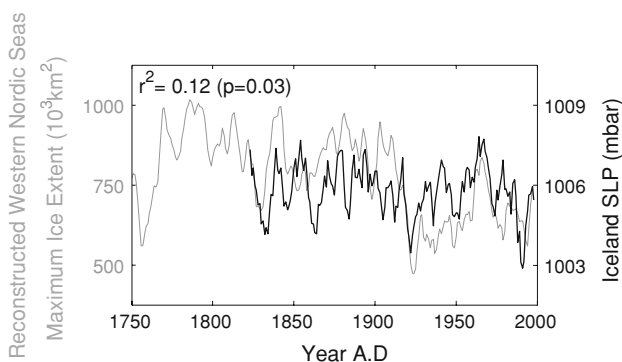


Fig. 7 Reconstructed maximum sea ice extent in the Western Nordic Seas (grey line) versus annual Iceland sea level pressure record since 1820 (black line; Jones et al. 1999). Significance level was calculated taking into account autocorrelation in the timeseries (see “Data and methods”)

(Jones et al. 1999) are indeed significantly correlated with our reconstruction (Fig. 7). Such situations enhance southerly warm winds over the Western Nordic Seas, causing: (1) compaction and reduced freezing in the ice margin (Vinje 2001), (2) warm air advection (Deser et al. 2000), and (3) enhanced flow of warm and saline Atlantic water (Grotefendt et al. 1998; Morison et al. 2000; Polyakov et al. 2004).

However, NAO/AO relationships with Arctic environment have been found to be far from stationary. Running correlation analyses showed near zero values between ice extent in the Western Nordic Seas and NAO winter index (Hurrell 1995; period 1864–1997) during 1860–1910s, negative and nearly significant correlations for 1920s–1950s ($p \sim 0.1$), and significant negative correlations ($p < 0.01$) since the 1950s (Fig. 8). This is also seen when comparing Iceland SLP and our sea ice reconstruction in the late nineteenth century–early twentieth (Fig. 7). Our finding agrees with previous reports on NAO-sea ice non-stationary relationships: whereas Nordic Seas sea ice has been reported to have strong negative correlation with NAO for the period 1957–1997 (Dickson et al. 2000) and significant correlations are reported between sea ice export in Fram Strait and AO or NAO since the late 1970s (e.g., Hilmer and Jung 2000), such relationships decay when analyzed over longer periods (e.g., Cavalieri 2002). For example, the rise of temperatures in the Arctic during the 1920–1940s was not related to the NAO (Bengtsson et al. 2004): AO and NAO were uncorrelated during this period, suggesting that atmospheric circulation patterns were in a reorganization phase then, possibly as a result of the sea ice

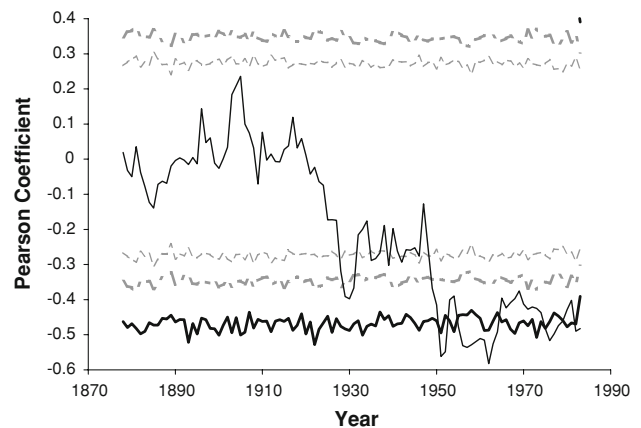


Fig. 8 Thin black line 30 year running correlation analysis of the relationship between winter NAO (Hurrell 1995) and sea ice extent in the Western Nordic Seas for the period 1864–1997, for which there is common data. Thick black line indicates significance at $p < 0.01$; discontinuous thick grey line indicates significance at $p < 0.05$, and discontinuous thin grey line indicates significance at $p < 0.1$. Significance levels were calculated taking into account autocorrelation in the timeseries (see “Data and methods”)

decrease (Jevrejeva and Moore 2001). This post-LIA reorganization hypothesis is supported by the good relationship between Iceland SLP and reconstructed sea ice extent in the early nineteenth century (Fig. 7). SATs, SSTs, and SLP over the North Atlantic during the period 1873–2000 have alternated decades of strong negative with decades of strong positive correlations with NAO (Polyakova et al. 2006). Likewise, NAO versus SAT long records from Europe showed evident non-stationarities on decadal time-scales (Slonosky et al. 2001). Suggested mechanisms for such non-stationarities are the co-occurrence or otherwise of several AO/NAO-related SLP patterns (Maslanik et al. 2007b), or the planetary-scale SLP wave (Cavaliere 2002), which explain features important for sea ice in the Nordic Seas that are only partly linked to NAO/AO. The mechanisms driving decadal AO/NAO variability are yet to be understood (Polyakov et al. 2004).

For completeness we also examined relationships with sunspot and total solar irradiance, finding that the decadal variability in the reconstructed sea ice extent showed no agreement with these solar forcing series (results not shown).

4 Conclusions

1. Long-term variability of maximum sea ice extent in the Western Nordic Seas—Iceland, Norway and Greenland seas—was successfully reconstructed since A.D. 1200 using a combination of a regional tree-ring chronology from the timberline area in northern Fennoscandia and $\delta^{18}\text{O}$ from the Lomonosovfonna ice core in Svalbard. The reconstruction explained 59% of the variance in sea ice extent variability based on the calibration period 1864–1997 and was validated against independent records of sea ice extent in the region.
2. We calculated for the first time the significance of the reconstruction statistics (RE, CE), as well as correlation coefficients, using a method based on bootstrapping confidence intervals for a given statistic by simulating data from a parsimonious AR model.
3. The twentieth century sustained the lowest maximum sea ice extent values since A.D. 1200.
4. Low maximum sea ice extent also occurred over periods of some decades (e.g., mid-seventeenth and mid-eighteenth centuries, early fifteenth and late thirteenth centuries), with absolute values in some cases as low as the twentieth century ones, but these periods were in no case as persistent as in the twentieth century.
5. Largest maximum sea ice extent values occurred from the seventeenth to the nineteenth centuries, during the Little Ice Age, whereas relatively small areas were covered by sea ice during the sixteenth century.

Overall moderate sea ice extent occurred during thirteenth to fifteenth centuries.

6. Low frequency variability (probably linked to the non-linear interaction of the thermohaline circulation and extrinsic forcing) and NAO/AO dominated decadal and interdecadal variability in sea ice extent at ~ 50 –120 year (centred at ~ 70 –90 year) and ~ 7 –32 year frequency bands, respectively.
7. Both oscillations have occurred repeatedly during the reconstructed period A.D. 1200–1997.
8. Sea ice extent and NAO showed a non-stationary relationship: significant negative correlations occurred since 1920s and especially during the second half of the twentieth century, whereas no relationship was found during the period 1860–1910s.
9. Variability at centennial scales was also observed, but the length of the reconstructed series did not allow quantifying its overall importance on sea ice extent variability.
10. The presently low maximum sea ice extent in the Western Nordic Seas is unique over the last 800 years, and results from a sea ice decline started in late-nineteenth century after the Little Ice Age.
11. The Western Nordic Seas sea ice reconstruction can be downloaded from the website <http://www.helsinki.fi/science/dendro/>.

Acknowledgments This study was partially funded by the G8 Legacy Chair in Ecology given to Dr. E.A. Johnson at the University of Calgary (Canada). We want to thank all the people who in various ways helped to make the Lomonosovfonna ice-coring project possible. Logistical support came from NPI in Longyearbyen and financial support came from Norwegian Polar Institute and The Norwegian Research Council. We would also want to thank Dmitry Divine at the Norwegian Polar Institute in Tromsø (Norway) for his help and assessment on the quality of the Nordic Seas sea ice records. Finally, thanks also to all the people from various institutions in Finland who have helped in the development of the supra-long timberline tree-ring chronology. The Kone Foundation supported Samuli Helama.

References

- ACIA (2004) Impacts of a warming Arctic. Cambridge University Press, Cambridge
- Akaike H (1974) A new look at the statistical model identification. *IEEE Trans Automat Contr* 19(6):716–723
- Alexander MA, Bhatt U, Walsh J, Timlin M, Miller J, Scott J (2004) The atmospheric response to realistic Arctic sea ice anomalies in an AGCM during winter. *J Clim* 17(5):890–905. doi: [10.1175/1520-0442\(2004\)017<0890:TARTRA>2.0.CO;2](https://doi.org/10.1175/1520-0442(2004)017<0890:TARTRA>2.0.CO;2)
- Alexandersson H, Schmidth T, Iden K, Tuomenvirta H (1998) Long-term variations of the storm climate over NW Europe. *Glob Atmos Ocean Syst* 6:97–120
- Bengtsson L, Semenov VA, Johannessen OM (2004) The early twentieth-century warming in the Arctic—a possible mechanism. *J Clim* 17:4045–4057

- Briffa KR, Jones PD, Pilcher JR, Hughes MK (1988) Reconstructing summer temperatures in northern Fennoscandia back to A.D. 1700 using tree-ring data from Scots pine. *Arct Antarct Alp Res* 20(4):385–394
- Briffa KR, Jones PD, Bartholin TS, Eckstein D, Schweingruber FH, Karlen W, Zetterberg P, Eronen M (1992) Fennoscandian summers from A.D. 500: temperature changes on short and long timescales. *Clim Dyn* 7:111–119
- Briffa KR, Jones PD, Schweingruber FH, Karlen W, Shiyatov SG (1996) Tree-ring variables as proxy-climate indicators: problems with low-frequency signals. In: Jones PD, Bradley RS, Jouzel J (eds) *Climate variations and forcing mechanisms of the last 2000 years*. Springer, Berlin, pp 9–41
- Briffa KR, Osborn TJ, Schweingruber FH (2004) Large-scale temperature inferences from tree rings: a review. *Glob Planet Change* 40:11–26
- Burg JP (1978) A new analysis technique for time series data. In: Childers DG (ed) *Modern spectrum analysis*. IEEE Press, New York, pp 42–48
- Cavaliere DJ (2002) A link between Fram Strait sea ice export and atmospheric planetary wave phase. *Geophys Res Lett* 29(12):1614. doi:10.1029/2002GL014684
- Comiso JC (2006) Abrupt decline in the Arctic winter sea ice cover. *Geophys Res Lett* 33:L18504. doi:10.1029/2006GL027341
- Comiso JC, Nishio F (2008) Trends in the sea ice cover using enhanced and compatible AMSR-E, SSM/I, and SMMR data. *J Geophys Res* 113:C02S07. doi:10.1029/2007JC004257
- Comiso JC, Parkinson CL, Gersten R, Stock L (2008) Accelerated decline in the Arctic sea ice cover. *J Geophys Res* 35:L01703. doi:10.1029/2007GL031972
- Cook ER, Peters K (1981) The smoothing spline: a new approach to standardizing forest interior tree-ring width series for dendroclimatic studies. *Tree Ring Bull* 41:45–53
- Cubasch U, Voss R, Hegerl GC, Waszkewitz J, Crowley TJ (1997) Simulation of the influence of solar radiation variations on the global climate with an ocean atmosphere general circulation model. *Clim Dyn* 13:757–767
- Delworth TL, Mann ME (2000) Observed and simulated multidecadal variability in the Northern Hemisphere. *Clim Dyn* 16:661–676
- Deser C, Teng H (2008) Evolution of Arctic sea ice concentration trends and the role of atmospheric circulation forcing, 1979–2007. *Geophys Res Lett* 35:L02504. doi:10.1029/2007GL032023
- Deser C, Walsh JE, Timlin MS (2000) Arctic sea ice variability in the context of recent atmospheric circulation trends. *J Clim* 13:617–633
- Dickson RR, Meincke J, Malmberg SA, Lee AJ (1988) The great salinity anomaly in the northern North Atlantic 1968–1982. *Prog Oceanogr* 20:103–151
- Dickson RR et al (2000) The Arctic Ocean response to the North Atlantic oscillation. *J Clim* 13:2671–2696
- Divine DV, Dick C (2006) Historical variability of sea ice edge position in the Nordic Seas. *J Geophys Res* 111:C01001. doi:10.1029/2004JC002851
- Erlandsson S (1936) *Dendrochronological studies, report 23*. Stockholms Högskolas Geokronologiska Institutet, Uppsala
- Eronen M, Zetterberg P, Briffa KR, Lindholm M, Meriläinen J, Timonen M (2002) The supra-long Scots pine tree-ring record for Finnish Lapland. Part 1. Chronology construction and initial inferences. *Holocene* 12(6):673–680
- Fischer H, Werner M, Wagenbach D, Schwager M, Thorsteinsson T, Wilhelms F, Kipfstuhl J, Sommer S (1998) Little ice age clearly recorded in northern Greenland ice-cores. *Geophys Res Lett* 25:1749–1752
- Fritts HC (1962) An approach to dendroclimatology: screening by means of multiple regression techniques. *J Geophys Res* 67:1413–1420
- Fritts HC (1976) *Tree rings and climate*. Academic Press, London
- Fritts HC, Swetnam TW (1989) Dendroecology: a tool for evaluating variations in past and present forest environments. *Adv Ecol Res* 19:111–188
- Ghil M, Allen MR, Dettinger MD, Ide K, Kondrashov D, Mann ME, Robertson AW, Saunders A, Tian Y, Varadi F, Yiou P (2002) Advanced spectral methods for climatic time series. *Rev Geophys* 40(1):3–1–3–41. doi:10.1029/2000RG000092
- Gleissberg W (1944) A table of secular variations of the solar cycle. *Terr Magn Atm Electr* 49:243–244
- Grinsted A, Moore JC, Jevrejeva S (2004) Application of the cross wavelet transform and wavelet coherence to geophysical time series. *Nonlin Process Geophys* 11:561–566
- Grotedefendt K, Logemann K, Quadfasel D, Ronski S (1998) Is the Arctic Ocean warming? *J Geophys Res* 103(C12):27679–27687
- Hammer C, Johnsen SJ, Clausen HB, Dahl-Jensen D, Gundestrup N, Steffensen JP (2001) The paleoclimatic record from a 345-m long ice-core from the Hans Tausen Iskappe. *Meddelelser om Grønland Geoscience* 39:87–95
- Helama S, Lindholm M, Timonen M, Meriläinen J, Eronen M (2002) The supra-long Scots pine tree-ring record for Finnish Lapland. Part 2. Interannual to centennial variability in summer temperatures for 7,500 years. *Holocene* 12(6):681–687
- Hilmer M, Jung T (2000) Evidence for a recent change in the link between the North Atlantic oscillation and Arctic sea ice export. *Geophys Res Lett* 27:989–992
- Holmes RL (1983) Computer-assisted quality control in tree-ring dating and measurement. *Tree Ring Bull* 43:69–78
- Hurrell JW (1995) Decadal trends in the North Atlantic oscillation: regional temperatures and precipitation. *Science* 269:676–679
- Isaksson E et al (2001) A new ice-core record from Lomonosovfonna, Svalbard: viewing the 1920–1997 data in relation to present climate and environmental conditions. *J Glaciol* 47(157):335–345
- Isaksson E et al (2003) Ice cores from Svalbard—useful archives of past climate and pollution history. *Phys Chem Earth* 28:1217–1228
- Isaksson E et al (2005) Two ice-core $\delta^{18}\text{O}$ records from Svalbard illustrating climate and sea-ice variability over the last 400 years. *Holocene* 15(4):501–509
- Jevrejeva S, Moore JC (2001) Singular spectrum analysis of Baltic Sea ice conditions and large-scale atmospheric patterns since 1708. *Geophys Res Lett* 28:4503–4506
- Jevrejeva S, Moore JC, Grinsted A (2003) Influence of the Arctic oscillation and El Niño–Southern oscillation (ENSO) on ice conditions in the Baltic Sea: The wavelet approach. *J Geophys Res* 108(D21):4677. doi:10.1029/2003JD003417
- Jones PD, Mann ME (2004) Climate over past millennia. *Rev Geophys* 42:RG2002. doi:10.1029/2003RG000143
- Jones PD, Briffa KR, Barnett TP, Tett SFB (1998) High-resolution palaeoclimatic records for the last millennium: interpretation, integration and comparison with general circulation model control-run temperatures. *Holocene* 8(4):455–471
- Jones PD et al (1999) Monthly mean pressure reconstructions for Europe for the 1780–1995 Period. *Int J Climatol* 19:347–364. doi:10.1002/(SICI)1097-0088(19990330)19:4<347::AID-JOC363>3.0.CO;2-S
- Kalnay E et al (1996) The NCEP/NCAR 40-year reanalysis project. *Bull Am Meteorol Soc* 77:437–471
- Kekonen T, Moore J, Perämäki P, Mulvaney R, Isaksson E, Pohjola V, van de Wal RSW (2005) The 800 year long ion record from the Lomonosovfonna (Svalbard) ice core. *J Geophys Res* 110:D07304. doi:10.1029/2004JD005223
- Knight JR, Allan RJ, Folland CK, Vellinga M, Mann ME (2005) A signature of persistent natural thermohaline circulation cycles in

- observed climate. *Geophys Res Lett* 32:L20708. doi:[10.1029/2005GL024233](https://doi.org/10.1029/2005GL024233)
- Lamb HH (1977) *Climate: present, past and future vol 2: climatic history and the future*. Methuen, London
- Lemke PJ, Ren J, Alley RB, Allison I, Carrasco J, Flato G, Fujii Y, Kaser G, Mote P, Thomas RH, Zhang T (2007) Observations: changes in snow, ice and frozen ground. In: Solomon S, Qin D, Manning M, Chen Z, Marquis M, Averyt KB, Tignor M, Miller HL (eds) *Climate change 2007: the physical science basis contribution of working group I to the fourth assessment report of the intergovernmental panel on climate change*. Cambridge University Press, Cambridge, pp 337–383
- Lindholm M (1996) Reconstruction of the past climate from ring-width chronologies of Scots pine (*Pinus sylvestris* L.) at the northern forest limit in Fennoscandia. Ph.D. Dissertation, University of Joensuu, Finland
- Lindsay RW, Zhang J (2005) The thinning of arctic sea-ice, 1988–2003: have we passed a tipping point? *J Clim* 18:4879–4894
- Lockwood M, Fröhlich C (2007) Recent oppositely directed trends in solar climate forcings and the global mean surface air temperature. *Proc R Soc A* 463:2447–2460. doi:[10.1098/rspa.2007.1880](https://doi.org/10.1098/rspa.2007.1880)
- Lorenz EN (1956) Empirical orthogonal functions and statistical weather prediction. MIT statistical forecasting project report no. 1, contract AF 19, 604–1566
- Løyning TB, Dick C, Goodwin H, Pavlova O, Vinje T, Kjærli G, Villinger T (2003) ACSYS historical ice chart archive (1553–2002). ACSYS IACPO informal report no. 8. World climate research programme, Arctic Climate System Study, Tromsø
- Magnusdottir G, Deser C, Saravanan R (2004) The effects of North Atlantic SST and sea ice anomalies on the winter circulation in CCM3. Part I. Main features and storm track characteristics of the response. *J Clim* 17(5):857–876
- Manabe S, Stouffer MJ, Stouffer RJ (1992) Transient responses of a coupled ocean–atmosphere model to gradual changes of atmospheric CO₂. Part II. Seasonal response. *J Clim* 5:105–126
- Mann ME, Emanuel K (2006) Atlantic Hurricane trends linked to climate change. *Eos Trans AGU* 87(24):233–244. doi:[10.1029/2006EO240001](https://doi.org/10.1029/2006EO240001)
- Mann ME, Rutherford S, Wahl E, Ammann C (2005) Testing the fidelity of methods used in proxy-based reconstructions of past climate. *J Clim* 18:4097–4107
- Maslanik JA, Fowler C, Stroeve J, Drobot S, Zwally J, Yi D, Emery W (2007a) A younger, thinner Arctic ice cover: increased potential for rapid, extensive sea-ice loss. *Geophys Res Lett* 34:L24501. doi:[10.1029/2007GL032043](https://doi.org/10.1029/2007GL032043)
- Maslanik JA, Drobot S, Fowler C, Emery W, Barry R (2007b) On the Arctic climate paradox and the continuing role of atmospheric circulation in affecting sea ice conditions. *Geophys Res Lett* 34:L03711. doi:[10.1029/2006GL028269](https://doi.org/10.1029/2006GL028269)
- Moberg A, Sonechkin DM, Holmgren K, Datsenko NM, Karlén W (2005) Highly variable Northern Hemisphere temperatures reconstructed from low- and high-resolution proxy data. *Nature* 433:613–617
- Moore GWK (2006) Reduction in seasonal sea ice concentration surrounding southern Baffin Island 1979–2004. *Geophys Res Lett* 33:L20501. doi:[10.1029/2006GL027764](https://doi.org/10.1029/2006GL027764)
- Moore JC, Grinsted A, Kekonen T, Pohjola V (2005) Separation of melting and environmental signals in an ice core with seasonal melt. *Geophys Res Lett* 32:L10501. doi:[10.1029/2005GL023039](https://doi.org/10.1029/2005GL023039)
- Moore J, Kekonen T, Grinsted A, Isaksson E (2006) Sulfate source inventories from a Svalbard ice core record spanning the industrial revolution. *J Geophys Res* 111:D15307. doi:[10.1029/2005JD006453](https://doi.org/10.1029/2005JD006453)
- Morison J, Aagaard K, Steele M (2000) Recent environmental changes in the Arctic: a review. *Arctic* 53(4):359–371
- Nghiem SV, Chao Y, Neumann G, Li P, Perovich DK, Street T, Clemente-Colón P (2006) Depletion of perennial sea ice in the East Arctic Ocean. *Geophys Res Lett* 33:L17501. doi:[10.1029/2006GL027198](https://doi.org/10.1029/2006GL027198)
- Nordli Ø, Kohler J (2003) *The early twentieth century warming. Daily observations at Green Harbor, Grønøfjorden, Spitsbergen*. Norwegian Meteorological Institute, Report No. 12/03 KLIMA, Oslo
- Ogilvie A (1992) Documentary evidence for changes in the climate of Iceland, A.D. 1500–1800. In: Bradley RS, Jones PD (eds) *Climate since A.D. 1500*. Routledge, London, pp 92–117
- Ogurtsov MG, Kocharov GE, Lindholm M, Meriläinen J, Eronen M (2002) Evidence of solar variation in tree-ring-based climate reconstructions. *Solar Phys* 205:403–417
- Overland JE, Wang M (2005) The Arctic climate paradox: the recent decrease of the Arctic oscillation. *Geophys Res Lett* 32:L06701. doi:[10.1029/2004GL021752](https://doi.org/10.1029/2004GL021752)
- Overpeck JK et al (1997) Arctic environmental change of the last four centuries. *Science* 278:1251–1256
- Parkinson CL, Cavalieri DJ (2008) Arctic sea ice variability and trends, 1979–2006. *J Geophys Res* 113:C07003. doi:[10.1029/2007JC004558](https://doi.org/10.1029/2007JC004558)
- Parkinson C, Cavalieri D, Gloersen P, Zwally H, Comiso J (1999) Arctic sea ice extents, areas, and trends, 1978–1996. *J Geophys Res* 104(C9):20837–20856
- Peterson BJ, Holmes RM, McClelland JW, Vorosmarty CV, Lammers RB, Shiklomanov AI, Shiklomanov IA, Rahmstorf S (2002) Increasing river discharge to the Arctic Ocean. *Science* 298:2171–2173
- Pohjola VA, Moore JC, Isaksson E, Jauhiainen T, van de Wal RSW, Martma T, Meijer HAJ, Vaikmäe R (2002) Effect of periodic melting on geochemical and isotopic signals in an ice core from Lomonosovfonna, Svalbard. *J Geophys Res* 107(D4):4036. doi:[10.1029/2000JD000149](https://doi.org/10.1029/2000JD000149)
- Polyakov IV, Johnson MA (2000) Arctic decadal and interdecadal variability. *Geophys Res Lett* 27(24):4097–4100
- Polyakov IV et al (2002) Observationally based assessment of polar amplification of global warming. *Geophys Res Lett* 29(18):1878. doi:[10.1029/2001GL011111](https://doi.org/10.1029/2001GL011111)
- Polyakov IV, Bekryaev RV, Alekseev GV, Bhatt US, Colony RL, Johnson MA, Makshtas AP, Walsh D (2003a) Variability and trends of air temperature and pressure in the Maritime Arctic, 1875–2000. *J Clim* 16:2067–2077
- Polyakov IV et al (2003b) Long-term ice variability in Arctic Marginal Seas. *J Clim* 16:2078–2085
- Polyakov IV et al (2004) Variability of the intermediate Atlantic water of the Arctic Ocean over the last 100 years. *J Clim* 17(23):4485–4497
- Polyakova EI, Journel AG, Polyakov IV, Bhatt US (2006) Changing relationship between the North Atlantic oscillation and key North Atlantic climate parameters. *Geophys Res Lett* 33:L03711. doi:[10.1029/2005GL024573](https://doi.org/10.1029/2005GL024573)
- Randall D et al (1998) Status of and outlook for large-scale modeling of atmosphere–ice–ocean interactions in the Arctic. *Bull Am Meteorol Soc* 79:197–219
- Rigor IG, Wallace JM, Colony RL (2002) Response of sea ice to the Arctic oscillation. *J Clim* 15:2648–2663
- Robinson DA, Serreze MC, Barry RG, Scharfen G, Kukla G (1992) Large-scale patterns and variability of snowmelt and parameterized surface albedo in the Arctic basin. *J Clim* 5:1109–1119
- Rothrock DA, Zhang J (2005) Arctic Ocean sea ice volume: what explains its recent depletion? *J Geophys Res* 110:C01002. doi:[10.1029/2004JC002282](https://doi.org/10.1029/2004JC002282)
- Rothrock DA, Yu Y, Maykut GA (1999) Thinning of the Arctic sea-ice cover. *Geophys Res Lett* 26:3469–3472

- Rothrock DA, Percival DB, Wensnahan M (2008) The decline in arctic sea-ice thickness: separating the spatial, annual, and interannual variability in a quarter century of submarine data. *J Geophys Res* 113:C05003. doi:[10.1029/2007JC004252](https://doi.org/10.1029/2007JC004252)
- Schaeffer M, Selten FM, Opsteegh JD, Goose H (2004) The influence of ocean convection patterns on high-latitude climate projections. *J Clim* 17:4316–4329
- Serreze MC, Francis JA (2006a) The Arctic amplification debate. *Clim Change* 76:241–264
- Serreze MC, Francis JA (2006b) The Arctic on the fast track of change. *Weather* 61(3):65–69
- Serreze MC, Carse F, Barry R, Rogers JC (1997) Icelandic low cyclone activity: climatological features, linkages with the NAO, and relationships with recent changes in the Northern Hemisphere circulation. *J Clim* 10:453–464
- Serreze MC et al (2000) Observational evidence of recent change in the northern high-latitude environment. *Clim Change* 46:159–207
- Serreze MC et al (2003) A record minimum arctic sea ice extent, area in 2002. *Geophys Res Lett* 30(3):1110. doi:[10.1029/2002GL016406](https://doi.org/10.1029/2002GL016406)
- Serreze MC, Holland MM, Stroeve J (2007) Perspectives on the Arctic's shrinking sea-ice cover. *Science* 315:1533–1536
- Shapiro I, Colony R, Vinje T (2003) April sea ice extent in the Barents Sea, 1850–2001. *Polar Res* 22(1):5–10
- Singarayer JS, Bamber J, Valdes PJ (2006) Twenty-first-century climate impacts from a declining Arctic Sea ice cover. *J Clim* 19:1109–1125
- Slonosky VC, Jones PD, Davies TD (2001) Atmospheric circulation and surface temperature in Europe from the eighteenth century to 1995. *Int J Climatol* 21:63–75
- Stroeve J, Holland MM, Meier W, Scambos T, Serreze M (2007) Arctic sea ice decline: faster than forecast. *Geophys Res Lett* 34:L09501. doi:[10.1029/2007GL029703](https://doi.org/10.1029/2007GL029703)
- Stroeve J, Serreze M, Drobot S, Gearheard S, Holland M, Maslanik J, Meier W, Scambos T (2008) Arctic Sea ice extent plummets in 2007. *Eos Trans AGU* 89(2):13–14
- Thompson DWJ, Wallace JM (1998) The Arctic oscillation signature in the wintertime geopotential height and temperature fields. *Geophys Res Lett* 25:1297–1300
- Thompson DWJ, Wallace JM (2000) Annular modes in the extratropical circulation. Part I. Month-to-month variability. *J Clim* 13:1000–1016
- Thompson DWJ, Wallace JM, Hegerl G (2000) Annular modes in the extratropical circulation. Part II. Trends. *J Clim* 13:1018–1036
- Torrence C, Compo GP (1998) A practical guide to wavelet analysis. *Bull Am Meteorol Soc* 79(1):61–78
- Tucker WB, Weatherly JW, Eppler DT, Farmer LD, Bentley DL (2001) Evidence for rapid thinning of sea ice in the Western Arctic Ocean at the end of the 1980s. *Geophys Res Lett* 28:2851–2854
- Vinje T (1976) Sea ice conditions in the European sector of the marginal seas of the Arctic, 1966–1975. *Norsk Polarinst, Årbok, 1975, Norwegian Polar Institute*, pp 163–174
- Vinje T (1999) Barents Sea ice edge variation over the past 400 years. Extended abstracts, workshop on sea-ice charts of the Arctic. World Meteorological Organization, Seattle, WMO/TD (949): 4–6
- Vinje T (2001) Anomalies and trends of sea-ice extent and atmospheric circulation in the Nordic Seas during the period 1864–1998. *J Clim* 14(3):255–267
- Vinnikov KY et al (1999) Global warming and Northern Hemisphere Sea ice extent. *Science* 286:1934–1937
- Vinther BM, Johnsen SJ, Andersen KK, Clausen HB, Hansen AW (2003) NAO signal recorded in the stable isotopes of Greenland ice cores. *Geophys Res Lett* 30(7):1387. doi:[10.1029/2002GL016193](https://doi.org/10.1029/2002GL016193)
- Virkkunen K, Moore JC, Isaksson E, Pohjola V, Perämäki P, Grinsted A, Kekonen T (2007) Warm summers and ion concentrations in snow: comparison of present day with Medieval Warm Epoch from snow pits and an ice core from Lomonosovfonna, Svalbard. *J Glaciol* 53(183):623–634
- Wigley TML, Briffa KR, Jones PD (1984) On the average value of correlated time series, with applications in dendroclimatology and hydrometeorology. *J Clim Appl Meteorol* 23:201–221
- Winton M (2006) Does the Arctic sea ice have a tipping point? *Geophys Res Lett* 33:L23504. doi:[10.1029/2006GL028017](https://doi.org/10.1029/2006GL028017)
- Zhang J, Lindsay R, Steele M, Schweiger A (2008) What drove the dramatic retreat of arctic sea ice during summer 2007? *Geophys Res Lett* 35:L11505. doi:[10.1029/2008GL034005](https://doi.org/10.1029/2008GL034005)